Deflection of a circular plate subjected to blast loading
by Larry Eugene May

A thesis submitted to the Graduate Faculty in partial fulfillment of the requirements for the degree of MASTER OF SCIENCE in Mechanical Engineering
Montana State University

Abstract:
The object of this investigation was to develop an analytical method for predicting the permanent deformation of a simply supported circular plate subjected to a blast loading. This development is based upon using the circular plate equations in conjunction with a hyperbolic tangent stress-strain relationship. The Modified Galerkin Method was used in obtaining solutions. The linear stress-strain relationship (Hooke's Law) was included to allow a comparison of results. The effects of strain rate sensitivity and time duration of blast loads upon deflection were also investigated.

By using the results of an experimental bomb blast test, a comparison of results was performed. From this comparison, it was found that by using the method developed, the plate deflections are greatly overestimated. This error results from using the plate equations which neglect the stretching effect upon the plate. Evidently, the energy absorbed by stretching is very significant when compared to the energy absorbed by bending.

1098-13
18

DEFLECTION OF A CIRCULAR PLATE SUBJECTED TO BLAST LOADING

by

LARRY EUGENE MAY

A thesis submitted to the Graduate Faculty in partial fulfillment of the requirements for the degree

of

MASTER OF SCIENCE

in

Mechanical Engineering

Approved:

Irvin L. Reis
Head, Major Department

Dennis O. Blackketter
Chairman, Examining Committee

K. Goering
Graduate Dean

MONTANA STATE UNIVERSITY
Bozeman, Montana

December, 1968

ACKNOWLEDGMENT

The author is indebted to the U. S. Army Ballistic Research Laboratories, Aberdeen Proving Ground, Maryland, for sponsoring this research project which provided the material for this thesis and financial aid.

The assistance of the following persons is gratefully acknowledged: Dr. Dennis O. Blackketter who directed this research project and provided guidance in the preparation of this thesis, Prof. George Frank for providing help in using the analog computer, and the author's wife, Carol, for typing this thesis.

TABLE OF CONTENTS

LIST OF TABLES

LIST OF FIGURES

ABSTRACT

The object of this investigation was to develop an analytical method for predicting the permanent deformation of a simply supported circular plate subjected to a blast loading. This development is based upon using the circular plate equations in conjunction with a hyperbolic tangent stress-strain relationship. The Modified Galerkin Method was used in obtaining solutions. The linear stress-strain relationship (Hooke's Law) was included to allow a comparison of results. The effects of strain rate sensitivity and time duration of blast loads upon deflection were also investigated.

By using the results of an experimental bomb blast test, a comparison of results was performed. From this comparison, it was found that by using the method developed, the plate deflections are greatly overestimated. This error results from using the plate equations which neglect the stretching effect upon the plate. Evidently, the energy absorbed by stretching is very significant when compared to the energy absorbed by bending.

CHAPTER I

INTRODUCTION AND STATEMENT OF PROBLEM

At the present there are no analytical methods available to accurately predict the permanent deformation of a simply supported plate subjected to blast loading. This blast loading may result in large deflections being experienced by the plate. In general, analytical solutions do not produce valid results since the equations of motion of the plate are based on small elastic deflection theory. This blast produces an impulse type loading when the time duration of the blast is much shorter than the fundamental mode of vibration of the plate.

When a plate undergoes large deflections resulting in the plate being stressed beyond the material yield point, the plate passes through the elastic deformation region into the plastic region. Thus, a complete solution of the plate deflection problem takes into account the deformation during the elastic region and the plastic region. Wang (1)* has derived the theoretical permanent deformation of a simply supported circular plate subjected to air blasts, which is based upon the "Plastic Rigid" theory he developed. In Wang's theory, a perfectly plastic-rigid material cannot deform when the stress is below the yield point, thus the elastic region is ignored. Some aluminum alloys approach this ideal plastic rigid condition.

---

* Numbers within a parenthesis refer to references.

Hoffman (2), in his thesis presented to the University of Delaware, used Wang's Plastic Rigid theory to calculate the permanent deformation of a 24 in. diameter simply supported 61S-T6 aluminum plate subjected to blast loading. He also performed blast tests to obtain the actual deformation, thus allowing a comparision. The stress-strain relationship for 61S-T6 aluminum can be interpreted as being plastic rigid. However, it was found by comparison of the theoretical results with experimental that the theoretical greatly overestimates the permanent deformation. This was true for the three different plate thicknesses used in his experiment; 1/8, 1/4, and 3/8 in.

This paper presents the development of an analytical method for calculating the deflection of a simply supported circular plate subjected to a bomb blast. This development consists of using the fundamental plate equation given by Timoshenko and Woinowsky-Krieger (3) in conjunction with a hyperbolic tangent stress-strain relationship. The Modified Galerkin Method was used to reduce the governing partial differential equation to a differential equation in time. By solving this differential equation, the plate deflection was obtained as a function of time. The development using the linear stress-strain relationship (Hooke's Law) was also performed to allow a comparison. It was assumed that the blast load was symmetric about the origin, thus reducing the problem to one dimension, and that all energy imparted to the plate was absorbed by the bending of the plate. A method for obtaining the permanent deformation from the deflection was not developed.

CHAPTER II

THEORETICAL ANALYSIS

2.1 Equilibrium Equation

The bending moment equilibrium equation for the symmetrical bending of a circular plate is given by Timoshenko and Woinowsky-Krieger (3) as

$$(1) \qquad \left[M_r + \frac{dM_r}{dr} r - M_t + Qr \right] dr\, d\theta = 0$$

Where M_r and M_t denote the radial and tangential bending moments per unit length, respectively. Q is the shearing force per unit length along the periphery of a cylindrical section. The equation for Q, developed by using the concept of equilibrium, includes both the surface load and the inertia effect (Figure 1).

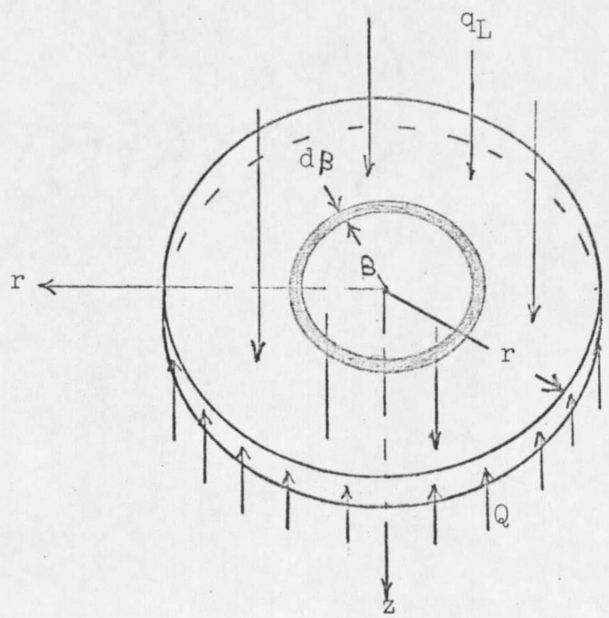

Fig 1. Cylindrical section of plate.

Thus, the resulting shear force per unit length is

$$(2) \quad Q = \frac{q_L r}{2} - \frac{\rho h}{rg} \int_0^r \left[\frac{\partial^2 w(\beta)}{\partial t^2}\right] \beta \, d\beta$$

with

β = distance to elemental section from origin.

q_L = uniform load on plate, psi.

ρ = density, lb/in^3.

h = plate thickness, in.

g = gravitational acceleration, in/sec^2.

$\frac{\partial^2 w}{\partial t^2}$ = second derivative of assumed deflection equation with respect to time, in/sec^2.

Timoshenko and Woinowsky-Krieger (3) developed the radial and tangential bending moments using the rectangular coordinate system and then converting to the polar coordinate system for the circular plate. However, in the development of the bending moments presented in this paper polar coordinates are used. The radial and tangential bending moments per unit length on the element are developed by taking the sum of the moments about the neutral axis (Figure 2). These bending moments per unit length are

$$(3) \quad M_r \, r d\theta = \int_{-h/2}^{h/2} z \, \sigma_r \, dz \, r d\theta$$

$$(4) \quad M_t \, dr = \int_{-h/2}^{h/2} z \, \sigma_t \, dz \, dr$$

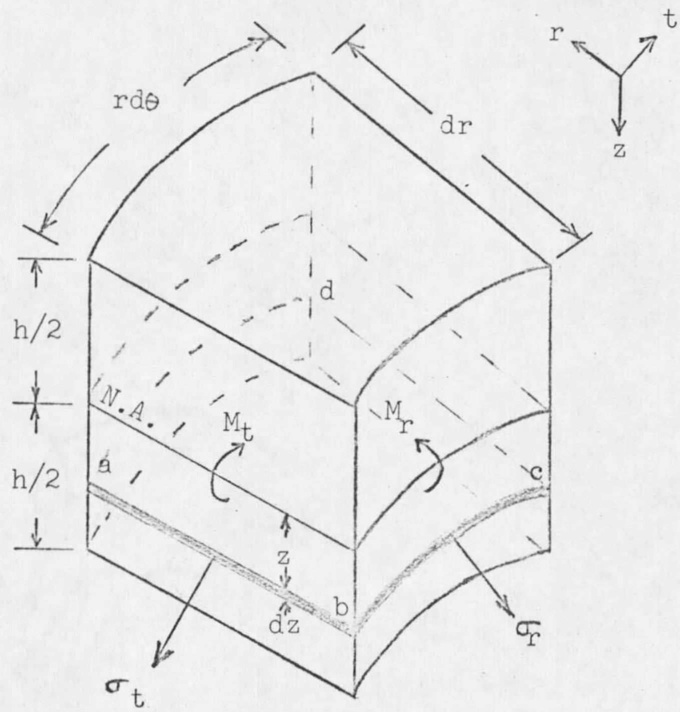

Fig 2. Element of circular plate.

Assuming that plane surfaces remain plane during bending of the plate, the unit elongations (strains) in the radial and tangential direction of the elemental lamina a b c d (Figure 2) at a distance z from the neutral axis are

$$(5) \quad \epsilon_r = \frac{z}{r_r}$$

(6) $\epsilon_t = \frac{z}{r_t}$

Where $1/r_r$ and $1/r_t$ are the principle curvatures of the circular plate in the radial and tangential directions, respectively. Timoshenko and Woinowsky-Krieger (3) present the following geometric relations

(7) $\frac{1}{r_r} = -\frac{\partial^2 w}{\partial r^2}$

(8) $\frac{1}{r_t} = -\frac{1}{r}\frac{\partial w}{\partial r}$

Where w is the deflection of the plate as shown in Figure 3. Partial derivatives are used since w is a function of both time and distance from the origin.

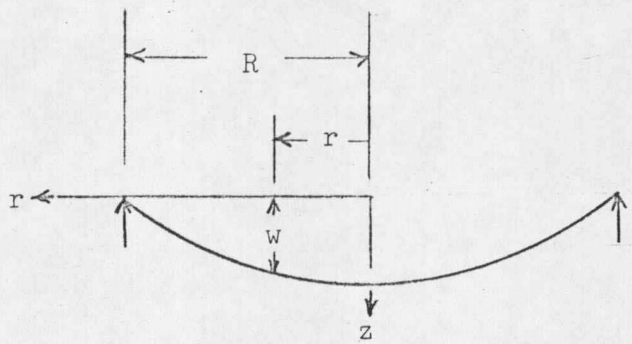

Fig 3. Simply supported circular plate.

2.2 Linear Stress-Strain Relationship

By using the linear stress-strain relationship, $\sigma = E\epsilon$, the stresses in the lamina a b c d of Figure 2 are

$$(9) \quad \sigma_r = \frac{E}{1-v^2}\left[\epsilon_r + v\epsilon_t\right]$$

$$(10) \quad \sigma_t = \frac{E}{1-v^2}\left[v\epsilon_r + \epsilon_t\right]$$

Where E represents the modulus of elasticity and v represents Poisson's ratio. After the substitution of Equations 5, 6, 7, 8, 9, and 10 into Equations 3 and 4 and integrating, the moment equations become

$$(11) \quad M_r = - \frac{E\ h^3}{12(1-v^2)}\left[\frac{\partial^2 w}{\partial r^2} + \frac{v}{r}\ \frac{\partial w}{\partial r}\right]$$

$$(12) \quad M_t = - \frac{E\ h^3}{12(1-v^2)}\left[v\ \frac{\partial^2 w}{\partial r^2} + \frac{1}{r}\ \frac{\partial w}{\partial r}\right]$$

Substituting Equations 2, 11, and 12 for Q, M_r and M_t into Equation 1, the equilibrium equation using the linear stress-strain relationship is

$$(13) \quad \left[\frac{E\ h^3}{12(1-v^2)}\left(-r\ \frac{\partial^3 w}{\partial r^3} - \frac{\partial^2 w}{\partial r^2} + \frac{1}{r}\ \frac{\partial w}{\partial r}\right) + \frac{q_L r^2}{2} - \frac{\rho h}{g}\int_0^r \frac{\partial^2 w(\beta)}{\partial t^2}\ \beta\ d\beta\right] dr d\theta = 0$$

2.3 Nonlinear Stress-Strain Relationship

The nonlinear stress-strain relationship used to approximate the actual stress-strain curve for the plate material is

$$(14) \quad \sigma = \frac{1}{b} \tanh a\epsilon$$

By varying the constants a and b, Equation 14, the initial slope and/or position of the stress-strain curve can be adjusted.

A discussion of difficulties which occur with other nonlinear stress-strain relationships which approximate the material stress-strain curve is given in Appendix A.

Hoffman (2) performed static tensile tests on the plate material, 61S-T6 aluminum, to obtain the material's stress-strain diagram. From this diagram, the average value of the yield stress was considered to be 41,000 psi. His diagram is shown in Figure 4 along with the curve for the hyperbolic tangent stress-strain relationship, Equation 14. With a yield point of 41,000 psi, the constants a and b are 303 (dimensionless) and 2.4×10^{-5} in^2/lb, respectively.

Since many materials are strain rate sensitive, it was decided to increase the yield points to 61,500 and 82,000 psi (Figure 4) to determine the effect of this phenomena upon plate deflection. The linear stress-strain curve is not strain rate sensitive. Strain rate tests (4) have been performed on aluminum 6061-T6 (previous alloy designation (5) 61S-T6) which show that this plate material is not strain rate sensitive for the range of strain rates expected in this analysis.

By using the nonlinear stress-strain relationship, Equation 14, the bending moments per unit length become

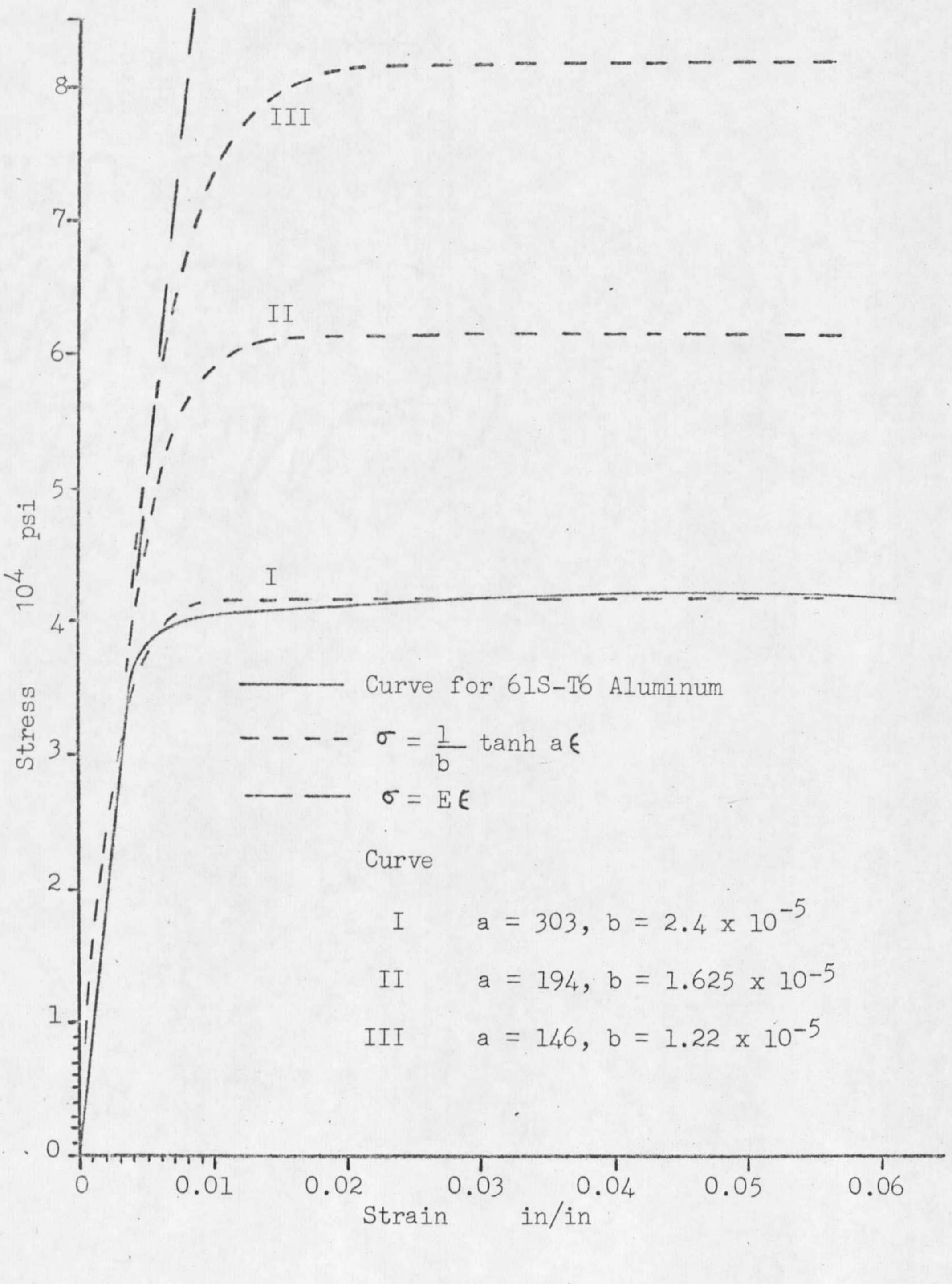

Fig 4. Stress-strain diagram.

$$(15) \qquad M_r = \frac{1}{b} \int_{-h/2}^{h/2} z \tanh Az \, dz$$

$$(16) \qquad M_t = \frac{1}{b} \int_{-h/2}^{h/2} z \tanh Bz \, dz$$

A and B are dependent upon the principle curvature of the plate, thus they are considered to be constants in the integration for the bending moments. The equations for A and B are

$$(17) \qquad A = - \frac{a}{1-v^2} \left[\frac{\partial^2 w}{\partial r^2} + \frac{v}{r} \frac{\partial w}{\partial r} \right]$$

$$(18) \qquad B = - \frac{a}{1-v^2} \left[v \frac{\partial^2 w}{\partial r^2} + \frac{1}{r} \frac{\partial w}{\partial r} \right]$$

Equations 15 and 16 were not directly integrated in this investigation because of the difficulties introduced by the hyperbolic tangent terms. It is possible to expand the hyperbolic tangent into a series and then integrate, but after the Modified Galerkin Method is applied, an unstable differential equation in time is obtained. To bypass these difficulties, it was decided to replace the z tanh zA term within the integral of Equation 15 with another function and then perform the necessary integration. It should be noted that Equations 15 and 16 are identical with the exception of constants A and B. By letting $X = Az$ and then replacing $X \tanh X$ with $\frac{-1 + \sqrt{1 + 5.64X^2}}{2}$ the bending moment becomes

$$(19) \qquad M_r = \frac{1}{bA^2} \int_{-Ah/2}^{Ah/2} \frac{-1 + \sqrt{1 + 5.64X^2}}{2} \, dx$$

Curves of X tanh X and $\frac{-1 + \sqrt{1 + 5.64X^2}}{2}$ are shown in Figure 5. By assuming that the 24 in. diameter plate undergoes a maximum center deflection of 3 inches, it is possible to estimate the values of the principle curvatures of the deflected plate. Then, by using Equations 7, 8, and 17, and a plate thickness of 1/4 in., the maximum value of Ah can be estimated to be 4.5, which results in $X_{max} = 2.25$. As shown in Figure 5, there is little difference between these two functions for $0 \leq X \leq 2.25$. Appendix B lists the magnitude of error between these two curves for $0 \leq X \leq 5$.

After integrating Equation 19, the bending moment per unit length is

$$(20) \qquad M_r = \frac{1}{2bA^2} \left[Ah \left(-1 + \tfrac{1}{2}\sqrt{1.41\ A^2h^2 + 1} \right) + 0.211 \ln \left(\frac{1.185\ Ah + \sqrt{1.41\ A^2h^2 + 1}}{-1.185\ Ah + \sqrt{1.41A^2h^2 + 1}} \right) \right]$$

Difficulties will again arise when applying the Modified Galerkin Method due to the natural logarithmic term in Equation 20. To eliminate these difficulties, this natural log term with the 0.211 constant was replaced by 0.33 Ah. This reduces Equation 20 to

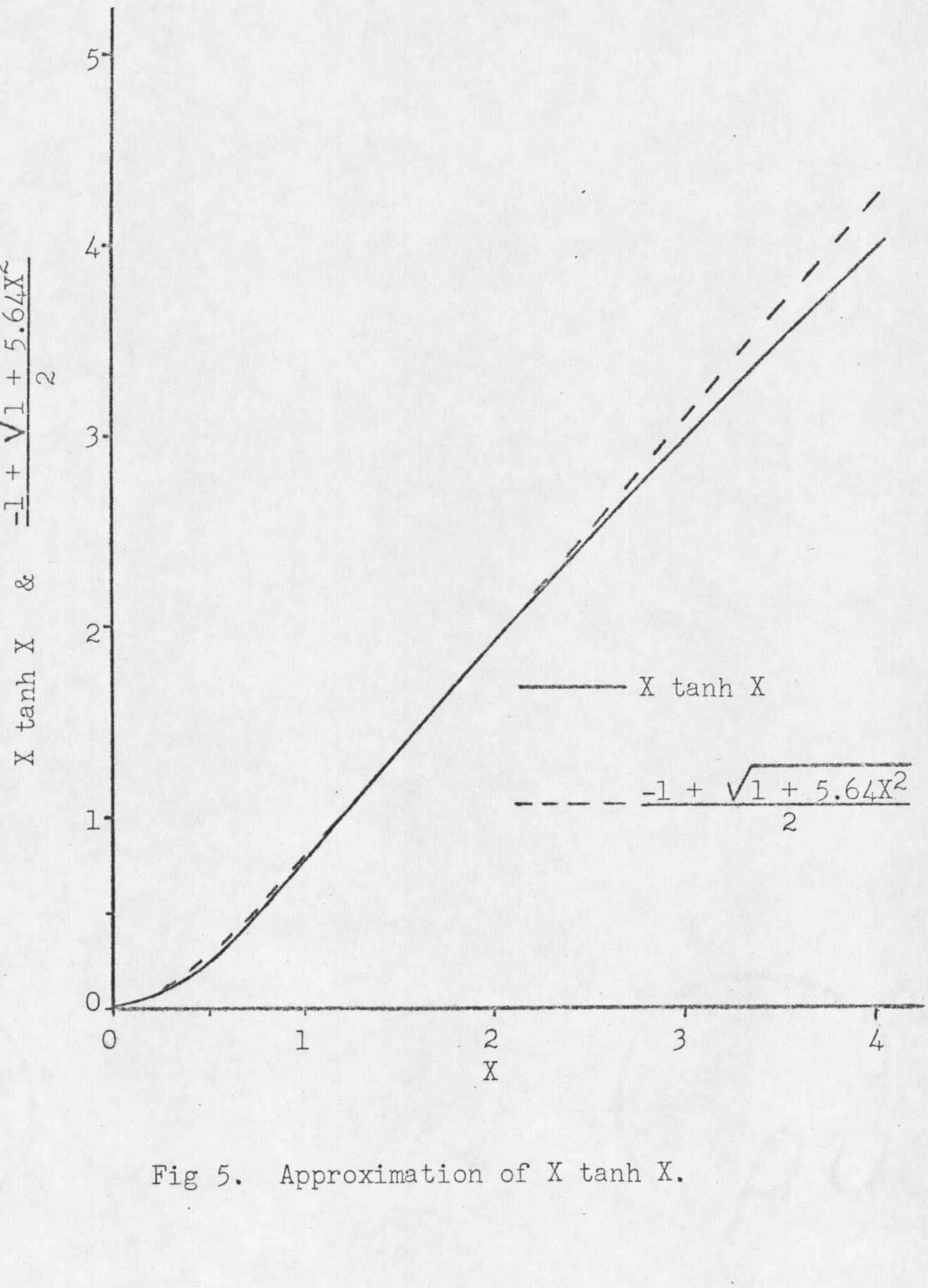

Fig 5. Approximation of X tanh X.

$$(21) \qquad M_r = \frac{1}{2bA^2}\left[-.67\ Ah + \frac{Ah}{2}\sqrt{1.41\ A^2h^2 + 1}\right]$$

Curves of $2bA^2M_r$ verses Ah for Equations 20 and 21 are plotted in Figure 6 to indicate the error resulting from this simplification. Appendix C lists the magnitude of this error for $0 \leq Ah \leq 5$.

The equation for M_t can be obtained by replacing A by B, thus

$$(22) \qquad M_t = \frac{1}{2bB^2}\left[-.67\ Bh + \frac{Bh}{2}\sqrt{1.41\ B^2h^2 + 1}\right]$$

After substituting Equations 17 and 18 into Equations 21 and 22, the bending moments become

$$(23) \qquad M_r = \frac{-h\ (1 - v^2)}{2ba\left(\frac{\partial^2 w}{\partial r^2} + \frac{1}{r}\frac{\partial w}{\partial r}\right)}\left\{-.67 + .5\left[\frac{1.41\ h^2a^2}{(1-v^2)^2}\left(\frac{\partial^2 w}{\partial r^2} + \frac{v}{r}\frac{\partial w}{\partial r}\right)^2 + 1\right]^{\frac{1}{2}}\right\}$$

$$(24) \qquad M_t = \frac{-h\ (1-v^2)}{2ba\left(v\frac{\partial^2 w}{\partial r^2} + \frac{1}{r}\frac{\partial w}{\partial r}\right)} \quad -.67 + .5\left[\frac{1.41h^2a^2}{(1-v^2)^2}\left(v\frac{\partial^2 w}{\partial r^2} + \frac{1}{r}\frac{\partial w}{\partial r}\right)^2 + 1\right]^{\frac{1}{2}}$$

Inserting Equations 2, 23, 24, and the first differential of Equation 23, into Equation 1, the equilibrium equation using the non-linear stress-strain relationship is

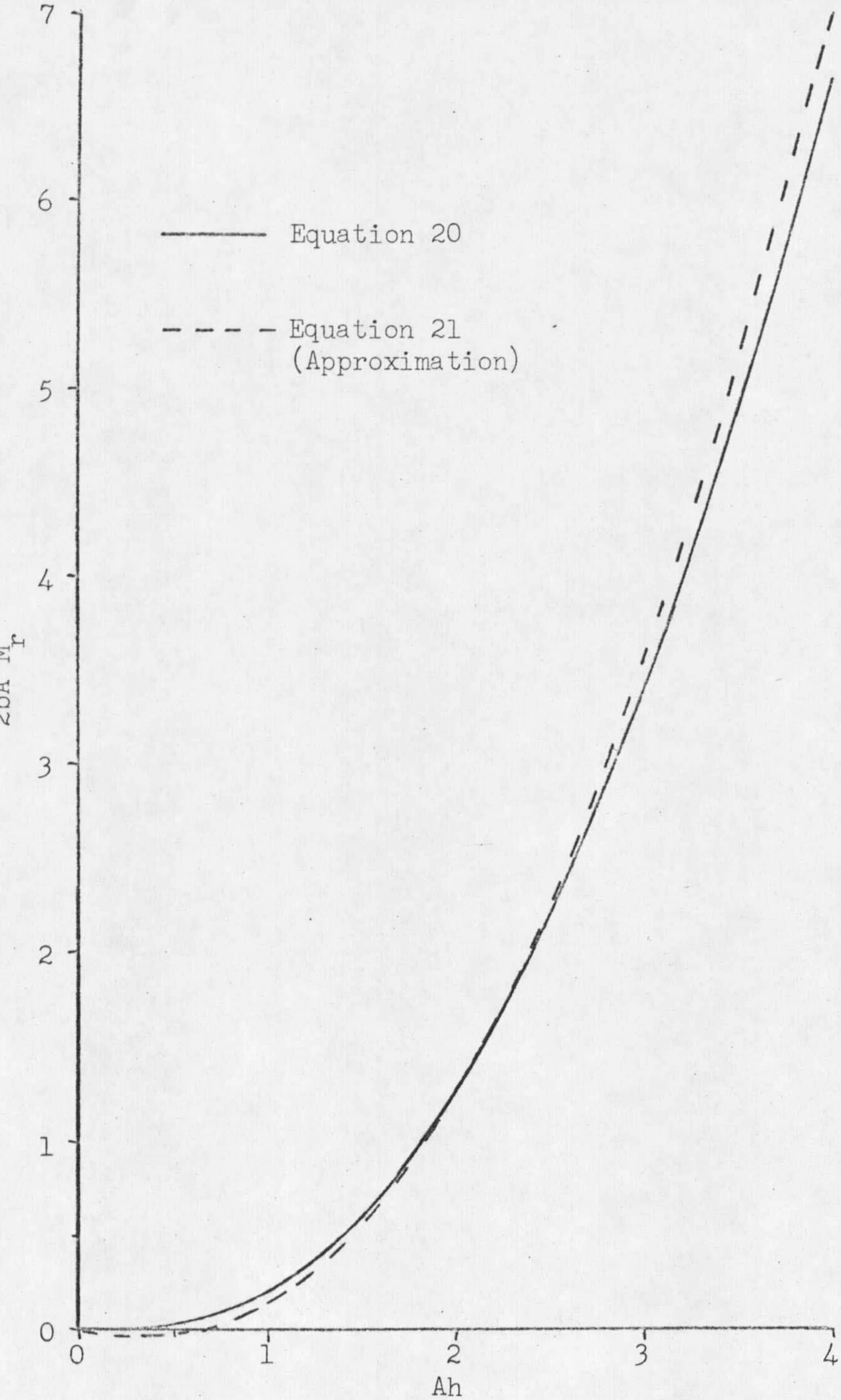

Fig 6. Curves of Equations 20 and 21

$$(25)\quad \Bigg\{ -\frac{h(1-v^2)}{2ba}\Bigg\{ \frac{-.67 + .5\left[\frac{1.41a^2h^2}{(1-v^2)^2}\left(\frac{\partial^2 w}{\partial r^2} + \frac{v}{r}\frac{\partial w}{\partial r}\right)^2 + 1\right]^{\frac{1}{2}}}{\frac{\partial^2 w}{\partial r^2} + \frac{v}{r}\frac{\partial w}{\partial r}}$$

$$+ r\left[\frac{.67 - .5\left[\frac{1.41a^2h^2}{(1-v^2)^2}\left(\frac{\partial^2 w}{\partial r^2} + \frac{v}{r}\frac{\partial w}{\partial r}\right)^2 + 1\right]^{\frac{1}{2}}}{\left(\frac{\partial^2 w}{\partial r^2} + \frac{v}{r}\frac{\partial w}{\partial r}\right)^2}\right.$$

$$\left. + \frac{1.41\,h^2a^2}{2(1-v^2)^2}\left[\frac{1.41\,a^2h^2}{(1-v^2)^2}\left(\frac{\partial^2 w}{\partial r^2} + \frac{v}{r}\frac{\partial w}{\partial r}\right)^2 + 1\right]^{-\frac{1}{2}}\right]\left[\frac{\partial^3 w}{\partial r^3}\right.$$

$$\left. + \frac{v}{r}\frac{\partial^2 w}{\partial r^2} - \frac{v}{r^2}\frac{\partial w}{\partial r}\right] + \frac{.67 - .5\left[\frac{1.41a^2h^2}{(1-v^2)^2}\left(v\frac{\partial^2 w}{\partial r^2} + \frac{1}{r}\frac{\partial w}{\partial r}\right)^2 + 1\right]^{\frac{1}{2}}}{v\frac{\partial^2 w}{\partial r^2} + \frac{1}{r}\frac{\partial w}{\partial r}}\Bigg\}$$

$$+ \frac{q_L r^2}{2} - \frac{\rho h}{g}\int_0^r \frac{\partial^2 w(\beta)}{\partial t^2}\,\beta\, d\beta \Bigg\}\, dr\, d\theta = 0$$

2.4 Application of Modified Galerkin Method

The Modified Galerkin Method (6, 7) was used to reduce the equilibrium equation to a differential equation in time. In using the Modified Galerkin Method, it is necessary to assume a solution to the equilibrium equation which satisfies the displacement boundary condition but not necessarily the force boundary conditions. If the assumed solution does not satisfy the force boundary conditions, the virtual work done on the boundary must be added to the virtual work done internal to the body. The Modified Galerkin Method requires that the virtual work done in each assumed mode of displacement be zero. In this circular plate problem, the assumed mode of displacement was a virtual rotation $\delta\left(\frac{\partial w}{\partial r}\right)$. The virtual work, W, done in this rotation can be written as

$$(26) \qquad W = \int_0^{2\pi}\int_0^R (\text{Equilibrium Equation})\ \delta\left(\frac{\partial w}{\partial r}\right)\Bigg|_{\substack{\text{internal}\\ \text{element}}}$$

$$+ \int_0^{2\pi} \left(M_B - M_r\right)\ \delta\left(\frac{\partial w}{\partial r}\right)\ r\ \Bigg|_{\substack{r=R\\ \text{surface}\\ \text{element}}} d\theta \ = 0$$

Where $M_B - M_r$ represents the bending moment equilibrium equation for the surface element, i.e. $R = r$. M_B is the external bending moment at $R = r$ and is zero for a simply supported plate.

One of the most critical steps in this investigation was the choosing of an assumed solution for the plate deflection. Such factors as the geometric shape taken by the plate, the displacement and force boundary conditions on the plate, and the assumed solution permitting the integration of Equation 26 were considered in making this choice. The assumed solution finally decided upon to represent the geometric shape taken by the plate due to blast loading is

$$(27) \qquad w = q\ (R^2 - r^2)$$

With q being a time dependent function. This assumed solution (Equation 27) does not satisfy the force boundary condition but does permit the integration of Equation 26 to be performed. The plate deflection at any point can be calculated using Equation 27.

By substitution of the radial bending moment and the equilibrium equation (Equations 11 and 13) which were developed using the linear stress-strain relationship, and the derivative of Equation 27 into Equation 26 a linear differential equation in time is obtained:

$$(28) \qquad \frac{\rho h R^4}{12g} \ddot{q} + \frac{h^3 E}{6(1-v)} q = \frac{q_L R^2}{8}$$

Similarly, by substituting the radial bending moment and equilibrium equation (Equations 23 and 25) developed by using the hyperbolic tangent stress-strain relationship, and the derivative of Equation 27 into Equation 26, a nonlinear differential equation in time is obtained:

$$(29) \qquad \frac{\rho h R^4}{12g} \ddot{q} + \frac{h(1-v)}{4\,ab} \frac{1}{q} \left[-.67 + .5 \sqrt{\frac{5.64\, h^2 a^2 (1+v)^2}{(1-v^2)^2} q^2 + 1} \right] = \frac{q_L R^2}{8}$$

The plate deflection can be calculated by first solving either Equation 28 or Equation 29 for q and then using Equation 27.

2.5 Loading Function

The applied load, q_L, was represented by an exponentially decaying function to similate a blast loading. The equation for q_L is

(30) $q_L = Pe^{-\lambda t}$

With P being the maximum pressure (psi) and λ being a time constant (1/sec).

In a bomb blast the pressure decreases with time to zero, goes negative and then returns to zero (8). The area under the negative portion of the curve is small when compared to the positive portion. When using an exponential decaying function, the negative portion of the curve is neglected. Note Figure 7 for a comparison of the two curves.

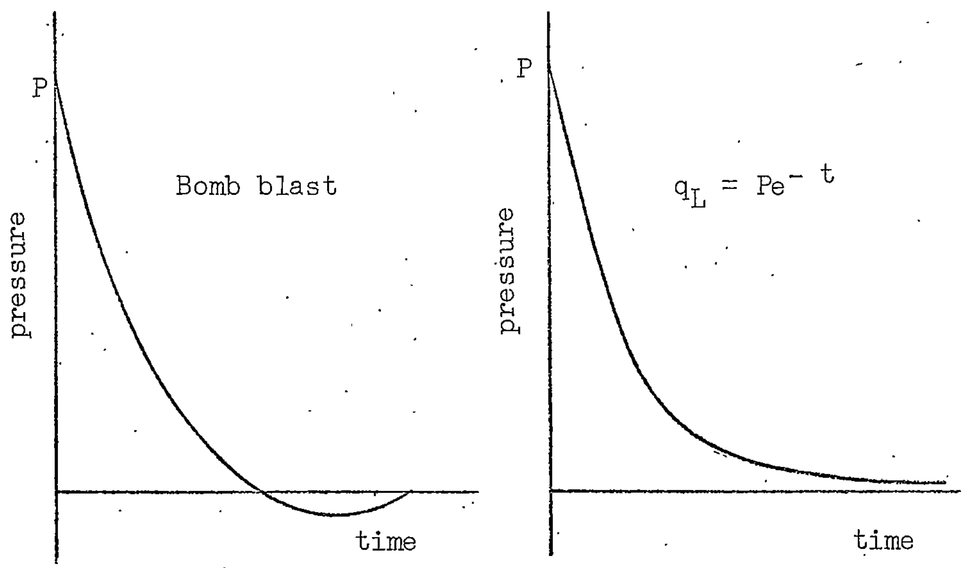

Fig 7. Pressure-time curve of blast.

Hoffman (2) states that the blast loading on the circular plate is essentially an impulse if the application of the load is much shorter than the fundamental elastic mode of vibration of the plate. This impulse, I, is equal to the area under the pressure-time curve. When the blast load is represented by an exponential decaying function, the impulse is given as

$$(31) \qquad I = \int_0^{\infty} P e^{-\lambda t}\, dt = \frac{P}{\lambda}$$

2.6 Analog Computer Method of Solving Differential Equations

To solve the linear and nonlinear second order differential equations, Equations 28 and 29, for q, an Electronic Associate, Inc. Pace TR-48 Analog Computer was used (9). The differential equations had to be magnitude scaled and time scaled to allow the use of the analog computer. By time scaling, the computer time was slowed down by a designated factor from the physical time. M denotes the magnitude of time scaling.

In solving the linear equation for q, Equation 28 was rearranged into the form

$$(32) \qquad \ddot{q} + C\, q = DP e^{-\lambda t}$$

with

$$C = \frac{h^2 E\ (2)\ g}{(1-v)\ \rho\ R^4}$$

$$D = \frac{12 g}{8 R^2 \rho\, h}$$

After magnitude scaling, Equation 32 becomes

$$(33) \quad -\left[\frac{\ddot{q}}{\ddot{q}_{max}}\right] = \frac{C}{\ddot{q}_{max}}\left[\frac{q}{q_{max}}\right] q_{max} - \frac{DP}{\ddot{q}_{max}} e^{-\lambda t}$$

Where $\ddot{q}_{max}$ and q_{max} are estimates of the maximum values of $\ddot{q}$ and q, respectively. The estimated maximum values of $\ddot{q}$ and q will correspond to 10 volts on the analog computer and were expressed in equation form as $\ddot{q}_{max} \approx DP$ and $q_{max} \approx \ddot{q}_{max} / C$. This is the unity method of scaling with 10 volts being the maximum voltage of the computer. The maximum value for $\dot{q}$ can be estimated to be half way between $\ddot{q}_{max}$ and q_{max}. The computer diagram used in solving the linear differential equation is given in Figure 8.

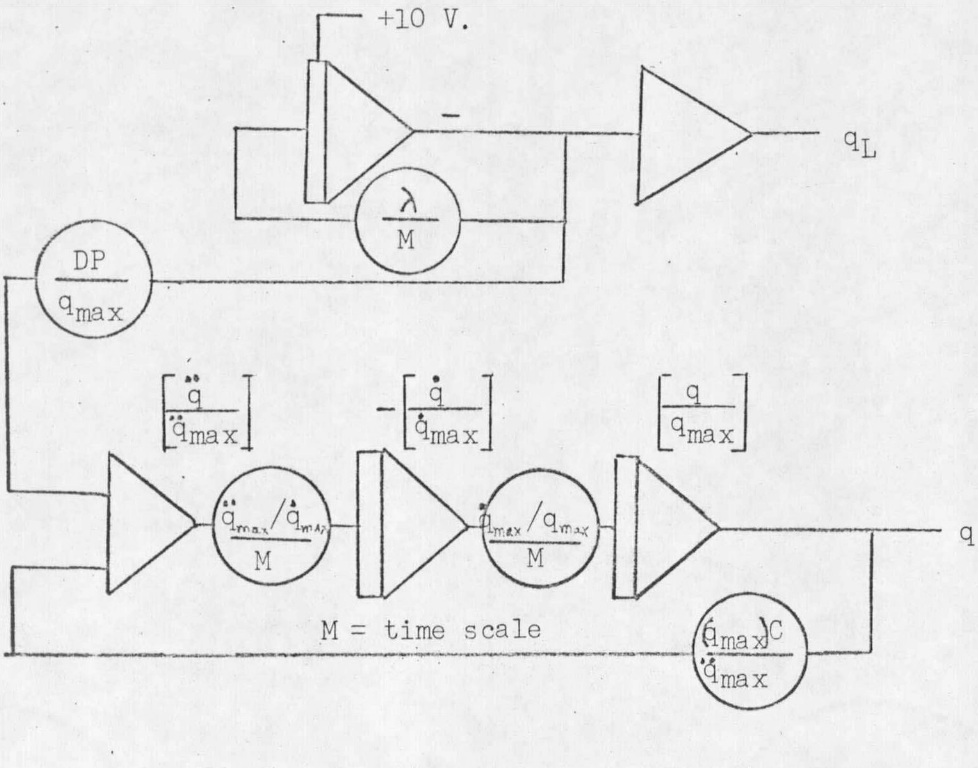

Fig 8. Computer diagram for Equation 33.

The same scaling method was used in programing the nonlinear equation on the computer as used for the linear equation. Equation 29 is rearranged into the following form:

$$(34) \qquad \ddot{q} + \frac{H}{q}\left[\sqrt{Fq^2 + 1} \quad - 1.34\right] = DP\, e^{-\lambda t}$$

with

$$H = \frac{3g\ (1-v)}{2\ ba\ \rho R^4}$$

$$F = \frac{5.64\ a^2h^2\ (1+v)^2}{(1-v^2)^2}$$

$$D = \frac{12g}{8\rho\ h\ R^2}$$

The resulting nonlinear scaled differential equation is

$$(35) \qquad -\left[\frac{\ddot{q}}{\ddot{q}_{max}}\right] = \frac{H}{\ddot{q}_{max}\ q_{max}}\ \frac{K}{\left[\frac{q}{q_{max}}\right]}\left(\sqrt{\frac{F}{K^2}\left[\frac{q}{q_{max}}\right]^2 q^2_{max} + \frac{1}{K^2}} - \frac{1.34}{K}\right) - \frac{DP}{\ddot{q}_{max}}\, e^{-\lambda t}$$

Where K was an arbitrary constant used to rearrange the magnitude of numbers. As in the linear case, $\ddot{q}_{max}$ (estimated) = 10 volts $\approx$ DP and q_{max} (estimated) = 10 volts $\approx \ddot{q}_{max}/C$. However, since the equation is nonlinear the maximum value of q may vary greatly from the estimated value of $\ddot{q}_{max}/C$, but this does provide a starting point. Again, $\dot{q}_{max}$ can be estimated to be half way between $\ddot{q}_{max}$ and q_{max}. The computer diagram used for the nonlinear equation is shown in Figure 9.

Time dependent plots of q and q_L were obtained by using an X - Y recorder in conjunction with the analog computer.

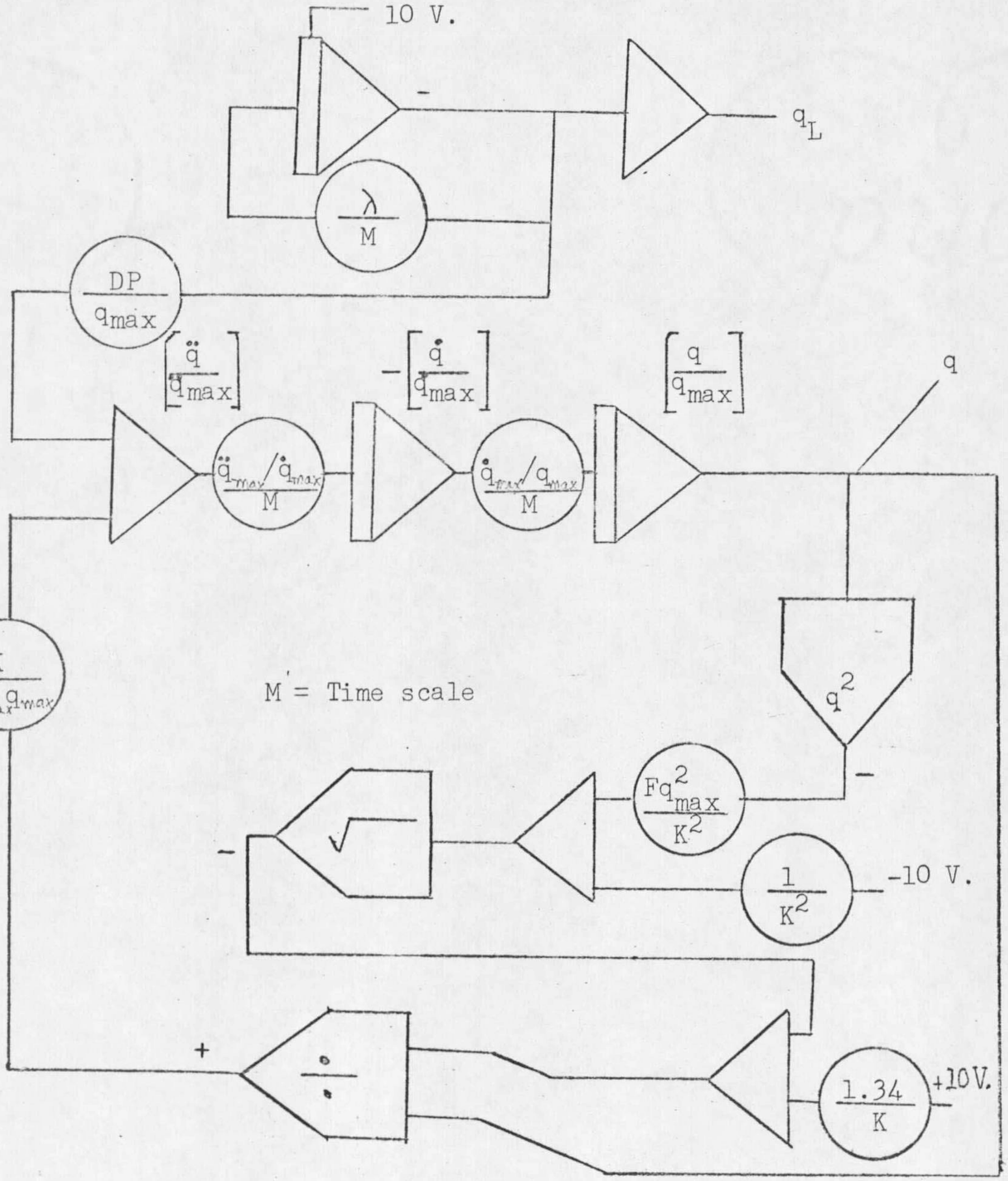

Fig 9. Computer diagram for Equation 35.

CHAPTER III

DEFLECTION OF CIRCULAR PLATE

3.1 Differential Equations

As discussed in Chapter II, the differential equations in time must be solved to obtain q as a function of time. By using the maximum value of q, the maximum deflection of the plate can be calculated. After rearranging Equations 28 and 29, the linear and nonlinear differential equations are

$$(36)\qquad \ddot{q} + \frac{2\ Eh^2\ g}{(1-v)\ \rho\ R^4}\ q = \frac{12g}{8R^2 \rho\ h}\ Pe^{-\lambda t}$$

$$(37)\qquad \ddot{q} + \frac{3g\ (1-v)}{2\ ab\ \rho\ R^4}\left(\frac{1}{q}\right)\left[\sqrt{\frac{5.64a^2h^2(1+v)^2}{(1-v^2)^2}\ q^2 + 1} - 1.34\right] = \frac{12g\ P e^{-\lambda t}}{8 \rho\ h\ R^2}$$

where

g, acceleration of gravity = 386 in/sec^2

E, modulus of elasticity = 10^7 psi

v, Poisson's ratio = 0.33

ρ, density = 0.098 lb/in^3

R, plate radius = 12 in.

The letters P, h, a, b, and λ represent variables which depend upon the configuration being studied. After substituting these constants into Equations 36 and 37, the linear and nonlinear equations become

$$(38)\qquad \ddot{q} + C\ q \equiv DPe^{-\lambda t} = Dq_L$$

$$\ddot{q} + \frac{H}{q}\left[\sqrt{Fq^2 + 1} - 1.34\right] = DPe^{-\lambda t} = Dq_L \tag{39}$$

respectively, where

$C = 5.67 \times 10^6 \quad h^2 \qquad (1/in^2 sec^2)$

$D = (41/h) \qquad (in^2/lb\ sec^2)$

$H = (0.191/ab) \quad (1/lb\ sec^2)$

$F = 12.58\ a^2 h^2$

It was decided to use one of Hoffman's (2) experimental impulses of I = 0.1483 psi-sec. to represent the blast loading. Hoffman, in his thesis, lists this impulse as 0.2075 psi-sec. However, since the writing of his thesis, more knowledge has been acquired in calculating impulses. In a recent telephone conversation Mr. Hoffman corrected the impulses given in his thesis and included the peak pressures for each impulse.

The analog computer was used to obtain solutions to Equation 38, for values of h, P, and λ as given in Table I. Also, the analog computer was used to obtain solutions to Equation 39 for values of h, P, λ, a, and b, as given in Table II. The values in Tables I and II were selected to demonstrate the effects of strain rate sensitivity, different peak pressures with constant total impulse, different impulses with constant peak pressures, and plate thickness upon the deflection of the plate.

TABLE I. Variables used in linear differential equation, $I = 0.1483$ psi-sec.

Run #	h in.	C (1/sec^2) x 10^5	P psi	λ 1/sec
1	1/4	3.55	20	135
2			50	337
3			50	674
4			100	674
5			100	1348
6			582	3920
7	3/8	7.96	100	674
8	1/8	0.885	10	67.4

TABLE II. Variables used in nonlinear differential equation, $I = 0.1483$ psi-sec.

RUN #	YIELD PT. psi	h in.	a	b $(in^2/lb) \times 10^{-5}$	D $in/lb\text{-}sec^2$	H $1/in^2 lb$	F $\times 10^4$	P psi	λ 1/sec
1	41,000	1/4	303	2.4	164	26.3	7.23	20	135
2								50	337
3								50	674
4								100	674
5								100	1348
6	61,500		194	1.625		60.6	2.96	50	337
7								50	674
8								100	674
9								100	1348
10	82,000		146	1.22		109.0	1.63	50	337
11								50	674
12								100	674
13								100	1348
14	41,000	3/8	303	2.4	109	26.3	16.21	100	674
15	41,000	3/8	303	2.4	328	26.3	1.805	10	67.4

3.2 Analog Computer Results

Figures 10 to 17 are curves of q verses time obtained by solving the differential equations on the analog computer. Also included in each of these figures is a curve of the loading function, q_L.

3.3 Plate Deflections

The maximum plate deflection was calculated using the maximum value of q and Equation 27, $w = q\ (R^2 - r^2)$, the assumed solution for the plate deflection that approximates the geometric shape taken by the plate after blast loading. All deflections presented in this paper are at the plate center, $r = 0$, since deflections at other points along the radius of the plate are not required in checking the validity of the analytical method developed in this paper. The calculated values of deflections are given in Table III.

3.4 Discussion of Analytical Results

In the following discussion, reference is made to the curves of q verses time, Figures 10 to 17; the plate deflection is directly proportional to the value of q.

As shown in Figure 10, with a plate thickness of 1/4 in., yield point of 41,000 psi, and $q_L = 20e^{-135t}$, using the nonlinear stress-strain relationship results in a smaller deflection (1.26 in.) than the linear relationship (2.38 in. deflection). This was expected since the non-linear stress-strain curve has a steeper slope at low stresses

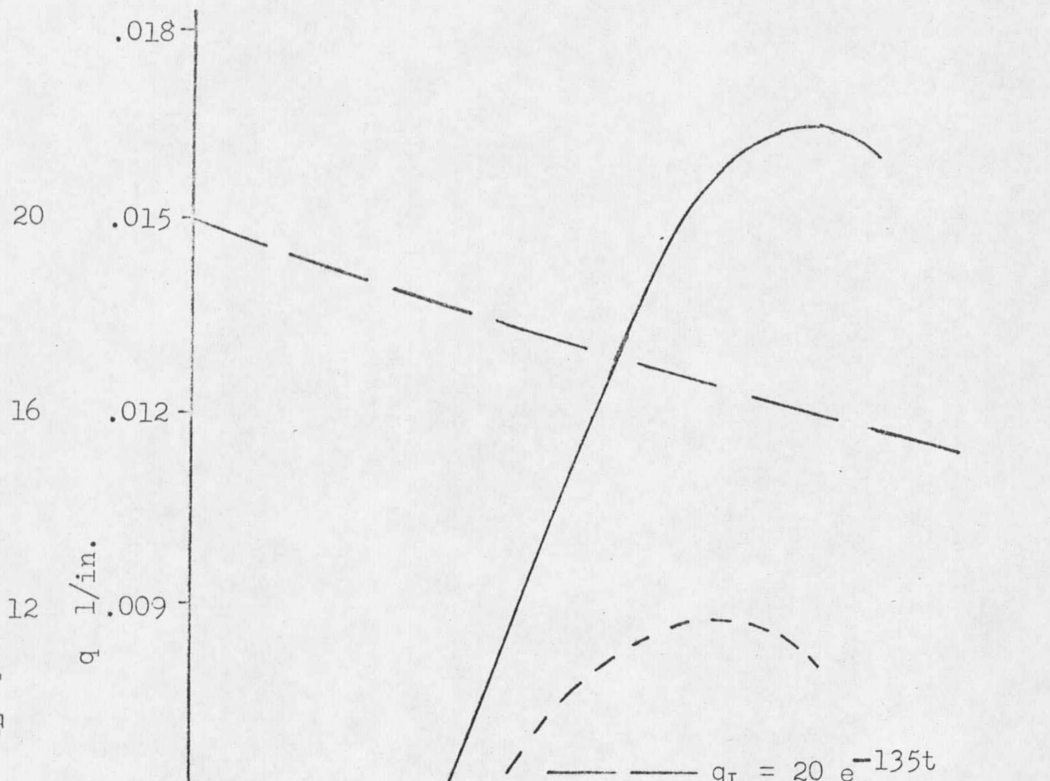

Fig 10. Curves of q and q_L; h = 1/4 in., $q_L = 20\ e^{-135t}$.

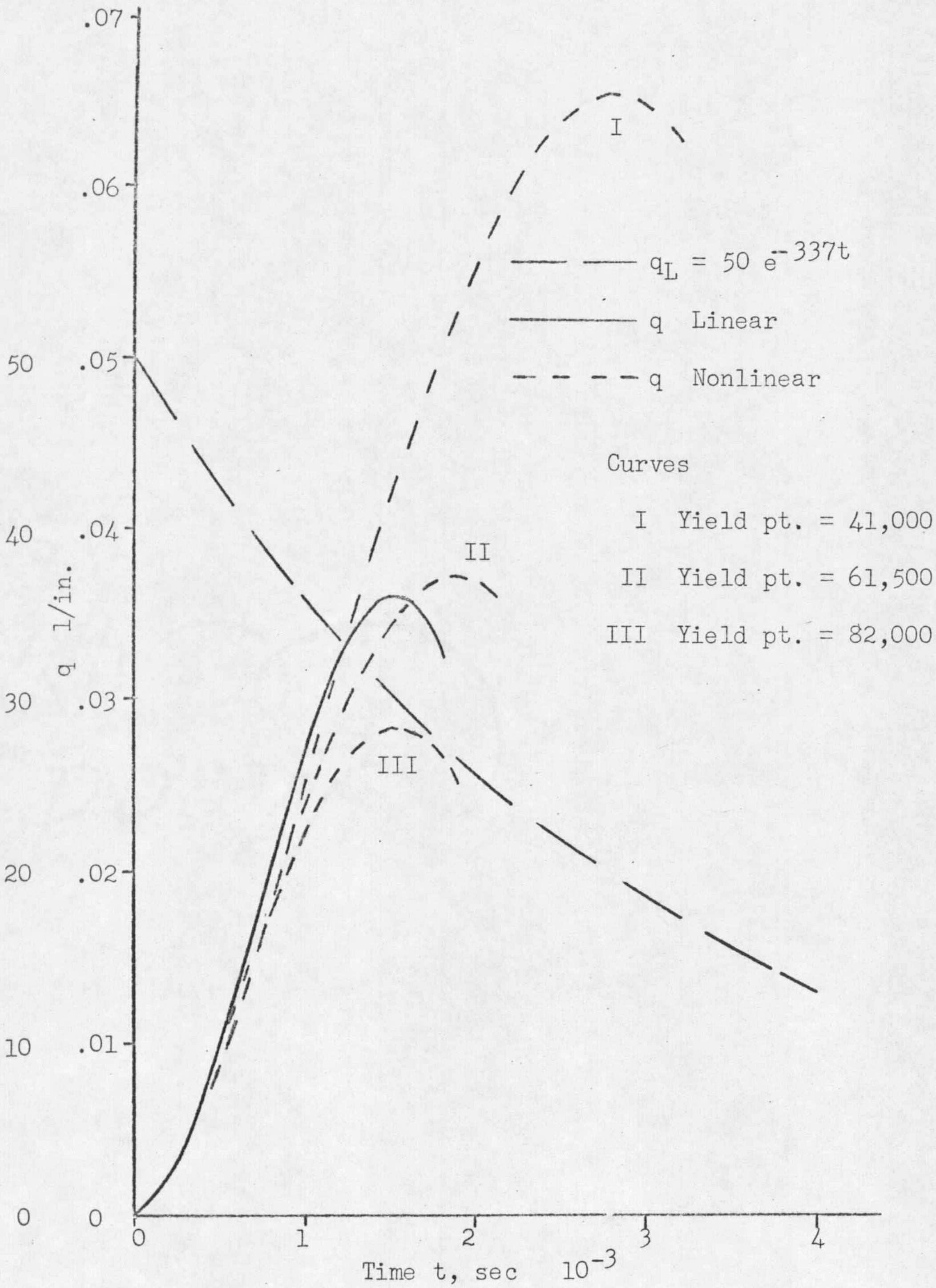

Fig 11. Curves of q and q_L; h = 1/4 in., $q_L = 50\ e^{-337t}$.

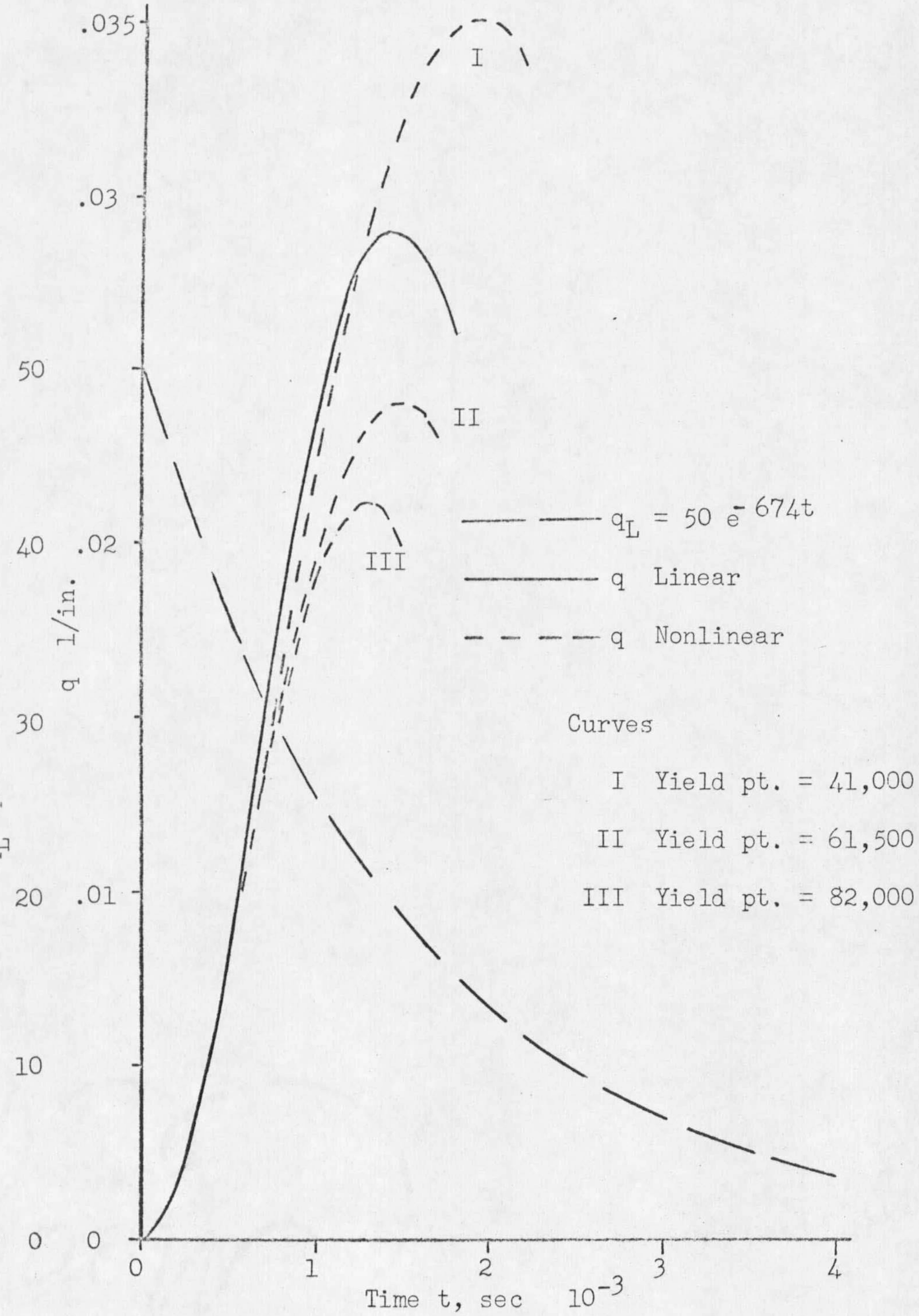

Fig 12. Curves of q and q_L; h = 1/4 in., $q_L = 50\ e^{-674t}$.

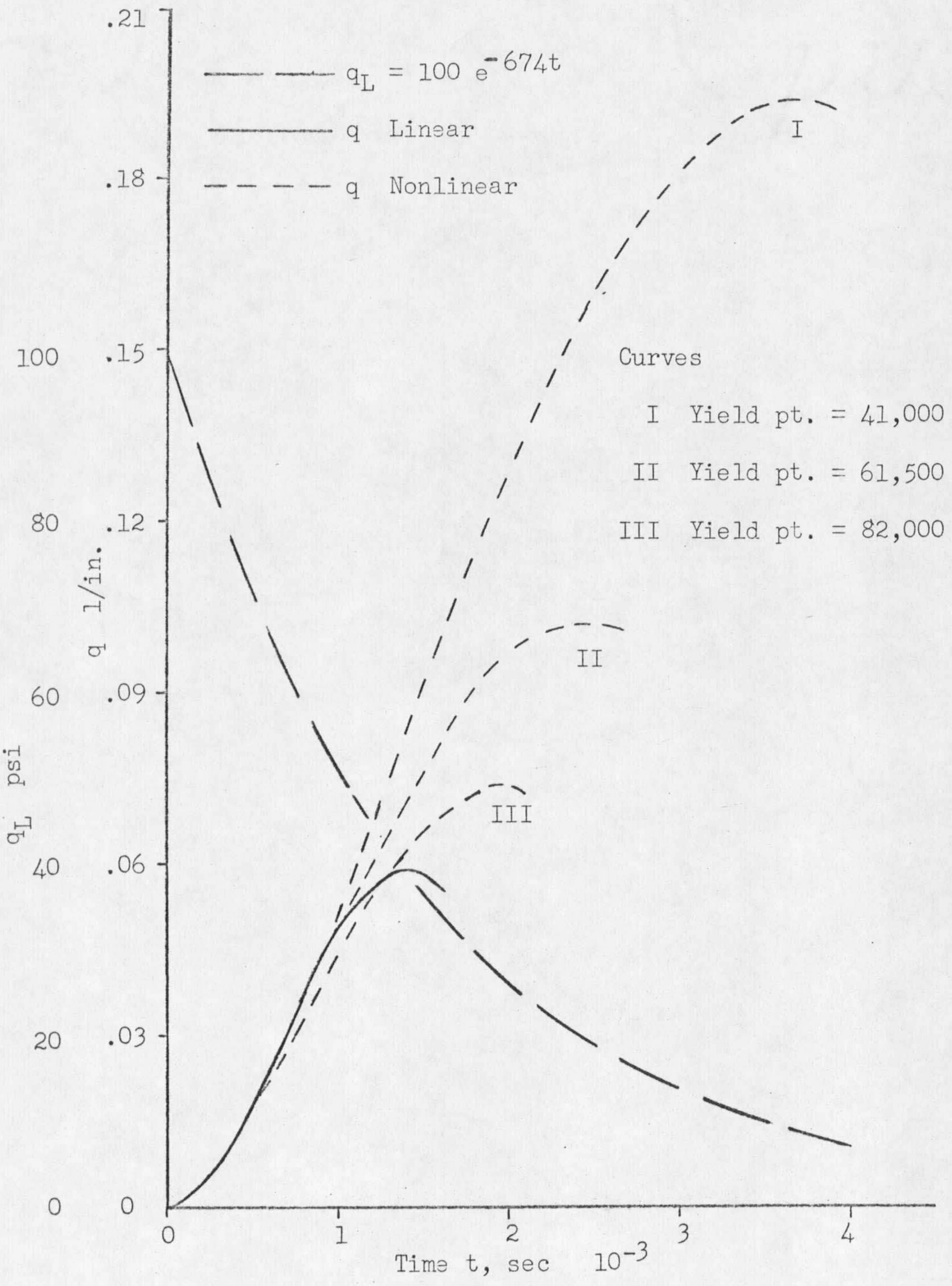

Fig 13. Curves of q and q_L; $h = 1/4$ in., $q_L = 100\ e^{-674t}$.

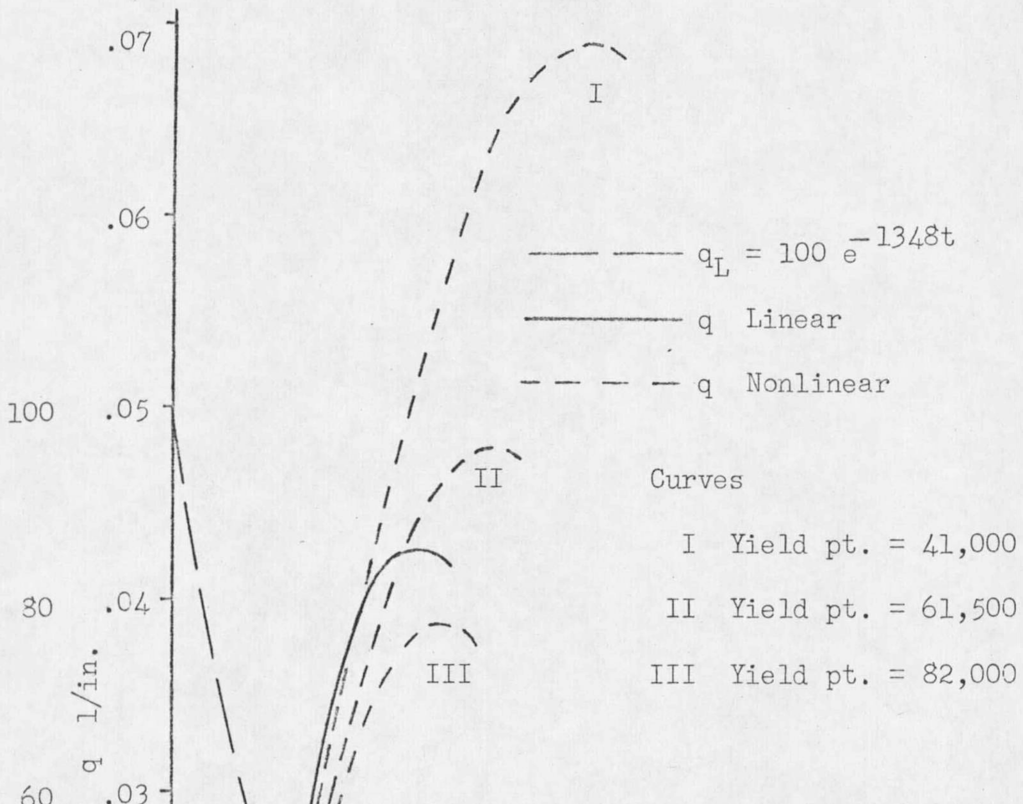

Fig 14. Curves of q and q_L; h = 1/4 in., $q_L = 100\ e^{-1348t}$.

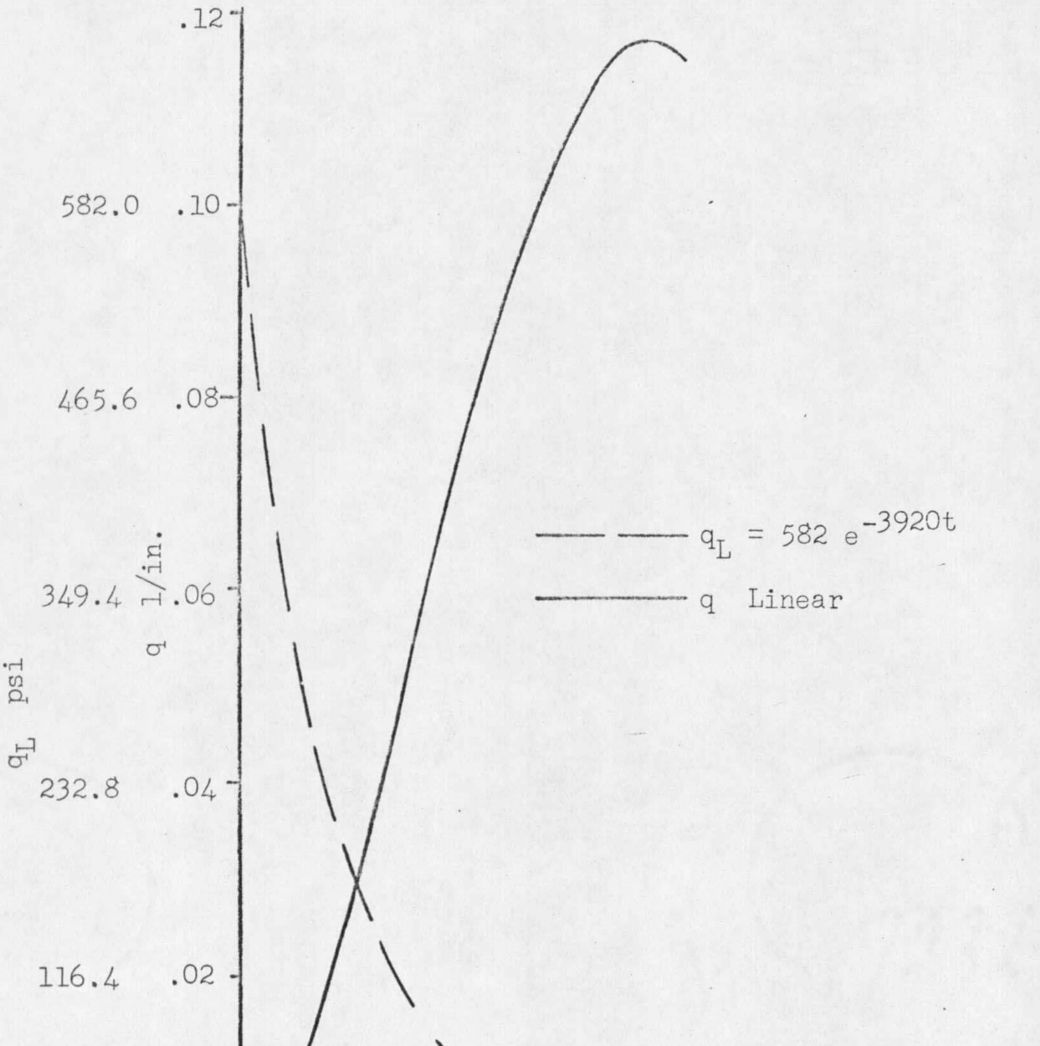

Fig 15. Curves of q and q_L; $h = 1/4$ in., $q_L = 582\ e^{-3920t}$.

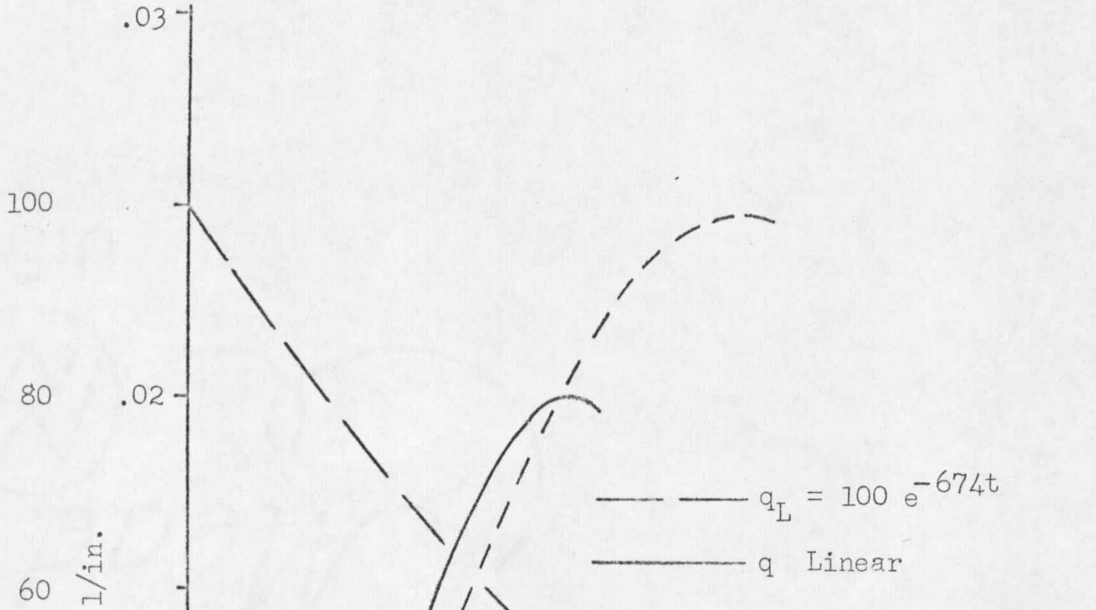

Fig 16. Curves of q and q_L; h = 3/8 in., $q_L = 100\, e^{-674t}$.

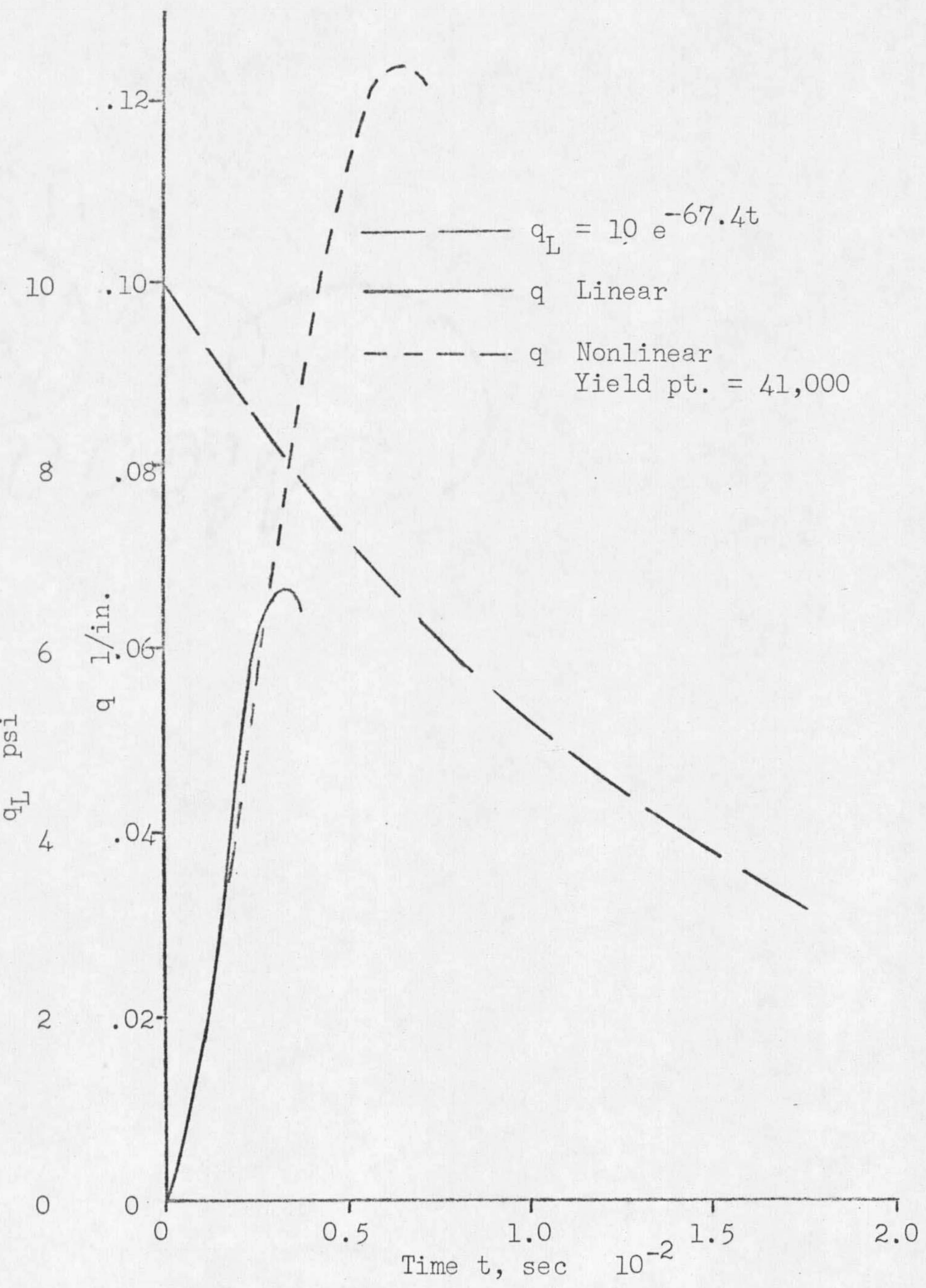

Fig 17. Curves of q and q_L; $h = 1/8$ in., $q_L = 10\ e^{-67.4t}$.

TABLE III. Deflections at center of plate

#	Yield Point psi	h 1/in	P psi	λ 1/sec	q_{max} 1/in.		Deflection w inches	
					Linear	Non-Linear	Linear	Non-Linear
1	41,000	1/4	20	135	0.0165	0.0088	2.38	1.265
2			50	337	0.036	0.0653	5.18	9.4
3			50	674	0.029	0.0353	4.18	5.09
4			100	674	0.0589	0.194	8.48	28.0
5			100	1348	0.0425	0.0692	6.12	9.95
6			582	3920	0.117	-	16.85	-
7	61,500		50	337	-	0.0372	-	5.35
8			50	674	-	0.024	-	3.46
9			100	674	-	0.105	-	15.12
10			100	1348	-	0.048	-	6.91
11	82,000		50	337	-	0.0283	-	4.07
12			50	674	-	0.021	-	3.02
13			100	674	-	0.0722	-	10.4
14			100	1348	-	0.0389	-	5.6
15	41,000	3/8	100	674	0.0200	0.0247	2.88	3.56
16	41,000	1/8	10	67.4	0.0662	0.124	9.52	17.88

(Figure 4) than the linear curve.

When loading functions of $50e^{-337t}$ and $100e^{-674t}$ are applied to the 1/4 in. plate using the nonlinear stress-strain relationship with a yield point of 41,000 psi results in plate deflection of 9.4 and 28 inches while the linear method results in plate deflections of 5.18 and 8.48 inches, respectively (Figures 11 to 14). At these high stresses the nonlinear stress-strain relationship creates a soft spring effect. Theoretically the strain could become infinite for stresses at the yield point using the hyperbolic tangent stress-strain relationship. It is physically impossible for a 24 in. diameter, 1/4 in. thick aluminum plate to deflect 28 in., or even 9 in., without undergoing a considerable amount of stretching. Yet, in the theory used in this investigation, all stretching effects were neglected. These very large deflections indicate that the energy absorbed in the stretching mode must be included.

When the loading function is increased to $582e^{-3920t}$ on the 1/4 in. thick plate, a solution to the nonlinear differential equation was not obtained. At this higher peak pressure of 582 psi, the equilibrium equation developed using the hyperbolic stress-strain relation requires that the maximum stress exceeds the possible values as dictated by the stress-strain relation causing the value of q to be indeterminate. However, a solution using the linear stress-strain relationship was obtained, which resulted in a plate deflection of 16.85 in.

The relationship between peak pressures and deflection for the 1/4 in. plate at a yield point of 41,000 psi is shown in Figure 18 for both the linear and nonlinear stress-strain method. These curves are similar to the stress-strain curves (Figure 4), which would be expected since the magnitude of the stress is proportional to the peak pressure, and the magnitude of the strain is proportional to the deflection.

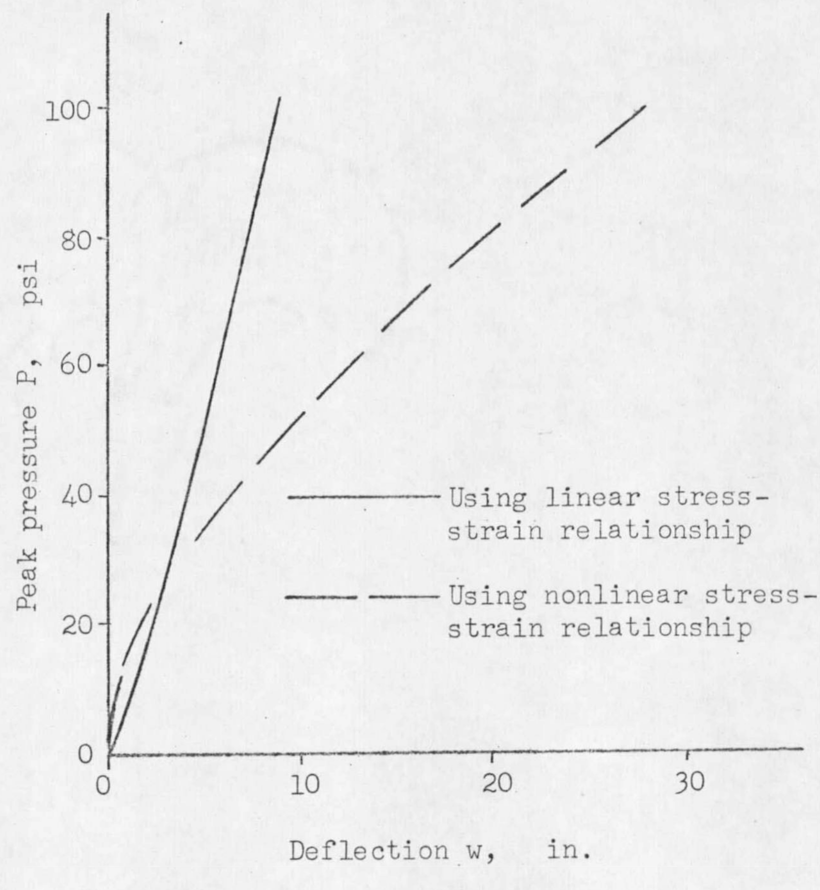

Fig 18. Peak pressure verses deflection; h = 1/4 in., constant total impulse.

The time duration, at a constant peak pressure, of the loading function effects the magnitude of the plate deflection. As an example, the deflection obtained by using the nonlinear stress-strain relation was 9.4 in. at $q_L = 50e^{-337t}$ and 5.09 in. at $q_L = 50e^{-674t}$. This effect of doubling the time duration was greater using a peak pressure of 100 psi as shown in Table III. One would expect this to happen since doubling the time constant reduces the impulse by 50 percent.

When the material yield point was increased, using the nonlinear stress-strain relationship, the plate deflection decreases as shown in Table III. To illustrate this, at $q_L = 100e^{-674t}$ and h = 1/4 in., the deflection was 28 in. at a yield point of 41,000 psi; at a yield point of 61,500 psi, the deflection was 15.12 in.; and at 82,000 psi the deflection was 10.4 in. Thus, if the plate material were strain rate sensitive, the magnitude of the deflection would be influenced. However, as previously mentioned, 61S-T6 aluminum was not strain rate sensitive but these tests were included to illustrate the strain rate sensitivity effect. If a material were strain rate sensitive, the deflection obtained by using the linear stress-strain relation would not be affected.

Increasing the plate thickness to 3/8 in. results in decreasing the magnitude of the deflection which would be expected. At $q_L = 100e^{-674t}$ the deflection was 2.88 and 3.56 in. obtained by using the linear and nonlinear stress-strain relationships, respectively.

With the same load and $h = 1/4$ in., the deflections were 8.48 (linear relationship) and 28 in. (nonlinear relationship). One test was performed with a plate thickness of 1/8 in. and $q_L = 10e^{-67.4t}$ (Figure 17) which resulted in plate deflections of 9.52 (linear) and 17.88 in. (nonlinear). At the same load of $10e^{-67.4t}$ and with $h = 1/4$ in., it was estimated, using Figure 18, that the deflection was 1.3 and 0.5 in. for the linear and nonlinear cases, respectively.

A curve of the loading function q_L is also included in Figures 10 to 17. Thus, the relationship between q_L and q can be readily seen.

The largest source of error in solving the equilibrium equations for the plate deflection will result from using the analog computer. Error as large as 20 percent is possible in using the analog computer to solve the nonlinear differential equation while error of less than 3 percent is likely to occur in solving the linear differential equation on the computer. A small source of error was the approximation of the X tanh X term and the natural logarithmic term with other functions in the development of the bending moments. However, it is unlikely that these errors resulted in such large plate deflections being obtained. These large plate deflections must be the result of neglecting the stretching effect upon the plate.

CHAPTER IV

ANALYTICAL AND EXPERIMENTAL RESULTS

4.1 Comparison of Analytical and Experimental Results

In one of Hoffman's (2) experimental tests using a 1/4 in. thick 24 in. diameter 61S-T6 aluminum plate with an impulse of 0.1483 psi-sec and a peak pressure of approximately 582 psi, a permanent deformation of 1.5 inches was obtained at the center of the plate. Using the Plastic Rigid theory developed by Wang (1), Hoffman calculated a permanent deformation at the plate center of 19.1 inches using the same plate thickness and loading function. In the investigation presented in this paper with the same test conditions ($I = 0.1483$ psi-sec., $P = 582$ psi, $h = 1/4$ in.) a deflection of 16.85 inches was calculated using the linear stress-strain relationship. As previously stated, the deflection was not obtained using the nonlinear stress-strain relation. Using the linear stress-strain relationship overestimates the actual plate deflection, but this one example resulted in a lower deflection than the value predicted by using the Plastic Rigid theory. Hoffman was dealing with permanent deformation while this investigation dealt with maximum deflection. The permanent deformation would be somewhat less than the deflection when the plate is stressed above the proportional limit.

By using the method developed in this paper with $h = 1/4$ in. and $q_L = 100e^{-674t}$ ($I = 0.1483$ psi-sec.), the nonlinear stress-strain relationship resulted in a deflection of 28 in. and the linear in a deflection of 8.48 inches. Yet, this peak pressure was 17.2 percent of Hoffman's 582 psi ($I = 0.1483$ psi-sec) with the actual permanent deformation of the plate being 1.5 in. at the center. The reason for using the hyperbolic stress-strain relationship was to enable obtaining a good approximation of the actual plate deformation. However, using this nonlinear stress-strain relation greatly overestimates the deflection at large loads. By using the linear stress-strain relationship the deflection was also overestimated but was less than the estimated value using the nonlinear relationship. Even in the case where the yield point was doubled, the nonlinear method greatly overestimates the deflection. A possible explanation for this overestimating is error in neglecting the stretching effect on the plate. The energy put into stretching must be very significant when compared to the energy absorbed by bending.

4.2 Conclusions

1. Plate theory is invalid for predicting the permanent deformation of a plate subjected to a bomb blast.

2. A valid solution might be obtained by using elasticity methods including both bending and stretching effects.

3. If a material is strain rate sensitive, this will influence the permanent deformations.

4. Changing the time duration of the blast with the peak pressure being held constant influences the permanent deformations of the plate.

APPENDIX

APPENDIX A

OTHER NONLINEAR STRESS-STRAIN RELATIONSHIPS

Other stress-strain relationships that were investigated are $\sigma = K\epsilon^n(10)$, $\sigma = E(\epsilon - a\epsilon^2)$, and $\sigma = 1/b \tan^{-1} a\epsilon$.

The relationship $\sigma = K\epsilon^n$ resulted in a poor approximation of the aluminum stress-strain curve. The initial slope of the stress-strain curve is zero, then it becomes very steep at small strains. This relationship also caused difficulties in integrating for the bending moments.

The nonlinear relationship $\sigma = E(\epsilon + a\epsilon^2)$, was unacceptable due to the resulting stress-strain curve. After the stress reached a maximum value, the slope of the stress-strain curve rapidly becomes increasingly negative.

The arctangent relationship, $\sigma = 1/b \tan^{-1} a\epsilon$, gives a fair approximation of the aluminum stress-strain curve. However, it was found that the hyperbolic tangent resulted in a much better approximation in the region where the actual curve bends over. Difficulties also arise in applying the Modified Galerkin Method when using the arctangent relationship.

APPENDIX B

ERROR ANALYSIS OF X TANH X APPROXIMATION

The following tabulation lists the error resulting from approximating X tanh X by $(-1 + \sqrt{1 + 5.64\, X^2})/2$ for $0 \leq X \leq 5$:

X	X tanh X	$(-1+ \sqrt{1+5.61X^2})/2$	Error
0.0	0.0	0.0	0.0
0.2	0.03947	0.05354	0.01405
0.4	0.15198	0.18963	0.03765
0.6	0.32223	0.37040	0.04817
0.8	0.53122	0.57349	0.04226
1.0	0.76159	0.78841	0.02681
1.2	1.00039	1.0101	0.00971
1.4	1.23949	1.23597	0.00352
1.6	1.47467	1.46459	0.01008
1.8	1.70425	1.69509	0.00916
2.0	1.92806	1.92693	0.00112
2.2	2.14663	2.15977	0.01314
2.4	2.36082	2.39337	0.03255
2.6	2.57147	2.62755	0.05608
2.8	2.77938	2.8622	0.08283
3.0	2.98516	3.09722	0.11205
3.2	3.18938	3.33254	0.14316
3.4	3.39243	3.56812	0.17568
3.6	3.59463	3.8039	0.20927
3.8	3.7962	4.03987	0.24367
4.0	3.99731	4.27598	0.27866
4.2	4.19811	4.51222	0.31411
4.4	4.39867	4.74858	0.34991
4.6	4.59907	4.9850	0.38596
4.8	4.79935	5.22157	0.42222
5.0	4.99954	5.45818	0.458641

APPENDIX C

ERROR ANALYSIS OF NATURAL LOG APPROXIMATION

The following is a tabulation of the error in the bending moment resulting from approximating 0.211 times the natural logarithmic term by 0.33 Ah:

Ah	Equation 20	Equation 21 (approximation)	Error
0.0	0.0	0.0	0.0
0.2	0.00187	-0.03121	0.03308
0.4	0.01453	-0.04658	0.06112
0.6	0.04731	-0.03364	0.08096
0.8	0.10739	0.01571	0.09168
1.0	0.19995	0.1062	0.09374
1.2	0.32864	0.24048	0.08816
1.4	0.49606	0.41999	0.07606
1.6	0.70402	0.64559	0.05243
1.8	0.95389	0.91776	0.03612
2.0	1.24666	1.23681	0.00984
2.2	1.5831	1.60293	0.01982
2.4	1.96379	2.01623	0.08761
2.6	2.38919	2.47681	0.08761
2.8	2.85968	2.98471	0.12502
3.0	3.37557	3.53999	0.16441
3.2	3.93709	4.14266	0.20557
3.4	4.54446	4.79277	0.2483
3.6	5.19785	5.49029	0.29244
3.8	5.89740	6.23528	0.33787
4.0	6.64325	7.02771	0.38445
4.2	7.4355	7.86762	0.43211
4.4	8.27424	8.75499	0.48074
4.6	9.15957	9.68983	0.53026
4.8	10.09155	10.67217	0.58062
5.0	11.07023	11.70197	0.63174

LITERATURE CONSULTED

1. Wang, A. J., "The Permanent Deflection of a Plastic Plate Under Blast Loading", Technical Report No. 7, Grad. Div. of Applied Math., Brown Univ., Dec., 1953.

2. Hoffman, A. J., "The Plastic Response of Circular Plates to Air Blasts", Master's Thesis, Dept. of Mech. Engr., Univ. of Delaware, June, 1955.

3. Timoshenko, S., and Woinowsky-Krieger, S., Theory of Plates and Shells, 2nd ed., McGraw-Hill, New York, 1959.

4. "Strain Rate Tests on Aluminum 6061-T6", GM Defense Research Laboratories, General Motors Corporation, TR65-69.

5. Baumeister, T. (Editor), Mechanical Engineers' Handbook, 6th ed., McGraw-Hill, New York, 1964.

6. Blackketter, D. O., "Two Dimensional Elasticity Problem by The Modified Galerkin Method", Technical Report No. 1, Dept. of Mech. Engr., Montana State Univ., May, 1968.

7. Anderson, R. A., Fundamentals of Vibrations, The Macmillan Company, New York, 1967.

8. Glasstone, S. (Editor), The Effects of Nuclear Weapons, Revised Edition, United States Atomic Energy Commission, April, 1962.

9. TR-48 Analog Computer Operators Manual, Electronic Associates, Inc., Long Branch, New Jersey, 1963.

10. Osgood, W. R., "Stress-Strain Formular", Journal of Aeronautical Sciences, January, 1946.